Ca^{2+}-Dependent Interaction with Calmodulin Is Conserved in the Synapsin Family: Identification of a High-Affinity Site†

Scott Nicol, Daisy Rahman, and Anthony J. Baines*

Research School of Biosciences, University of Kent, Canterbury, Kent, CT2 7NJ, England

Received March 26, 1997; Revised Manuscript Received June 20, 1997⊗

ABSTRACT: The synapsins are a family of proteins associated with small synaptic vesicles that are implicated in synaptic maintenance and in the supply of vesicles for exocytosis. They are well characterized as substrates for protein kinases, and one class of synapsin, synapsin I, has been shown to bind, and be regulated by, calmodulin. A representative of the synapsin II class is now shown to bind calmodulin. Optical biosensor assays of Ca^{2+}-dependent calmodulin binding to recombinant rat synapsin IIb indicated an apparent K_D for calmodulin of 31 ± 5 nM. Phosphorylation at Ser 10 increased the rates of calmodulin association (by a factor of 10) and dissociation (by a factor of 20). Fragment analysis and predictions from the sequence indicated two potential calmodulin binding sequences in the conserved central (C) domain. Peptides representing these sequences (residues 122−143 and 313−334 in synapsin IIb) were synthesized. Peptide 122−143 was found to bind calmodulin (K_D 32 ± 10 nM) and inhibit interaction of synapsin IIb with calmodulin. The interaction of peptide 313−334 was much weaker. Sequences similar to residues 122−143 are present in all published synapsin sequences. Calmodulin binding by synapsins seems not to be confined to mammals: a recombinant *Drosophila* synapsin 1 fragment containing part of the C-domain showed Ca^{2+}-dependent binding to mammalian calmodulin. We conclude that calmodulin binding to synapsins is likely to be a general aspect of regulation of synaptic function.

The formation and retention of synapses and their exocytotic function are central to neurobiology. A family of proteins known as synapsins has been implicated in each of these processes. The mammalian synapsins are derived from two genes (I and II) that give rise to four protein products by differential mRNA splicing (Ia, polypeptide chain size 74 kDa; Ib, 70 kDa; IIa, 63 kDa; and IIb, 52 kDa) (*1*). These proteins are extremely abundant in mammalian synapses and are major targets for multiple protein kinases. Studies on transgenic mice carrying null mutations in one or both of the synapsin genes (*2*−*4*), and on cultured neurons treated with anti-sense oligonucleotides (*5*), have suggested that synapsins are required for normal synaptic organization. Synapsin null mice showed electrophysiological anomalies (*2*): the products of each gene were suggested to be essential for accelerating vesicle traffic during repeated stimulation. Recently, the synapsins in *Drosophila* have been molecularly cloned, which will open the path to more detailed genetic analyses of structure−function relationships in synapsins (*6*).

It appears that the synapsins' role is to cross-link small synaptic vesicles (SSV) to the cytoskeleton in presynaptic terminals. The synapsins are peripheral proteins of SSV membranes, capable of binding and cross-linking multiple cytoskeletal proteins—this is clearly illustrated by electron microscopy (*7*). The simplest hypothesis is that SSV are clustered within the presynaptic cytoplasm by being cross-linked to the cytoskeleton. Repeated stimulation of synapses would, in this hypothesis, lead to breaking of the vesicle−cytoskeleton bridges, and release of SSV for use in exocytosis. In the absence of one or other of the pairs of synapsin gene products, the mechanism for supplying vesicles during repeated stimulation would be dysfunctional, consistent with the electrophysiological anomalies [see Sudhof (*8*) for a review].

In previous work, we identified a novel mode of regulation of synapsin I activity by Ca^{2+}-dependent binding of calmodulin (*9*−*11*). Calmodulin regulates the interaction of synapsin I with F-actin: it suppresses binding of synapsin I to preformed actin filaments, and bundling of actin filaments by synapsin I. Moreover, calmodulin binding and phosphorylation of synapsin I act together to control the interactions of synapsin I: phosphorylation potentiates some of the effects of calmodulin. Binding of calmodulin occurs within the N-terminal 'head' region of synapsin I: high-affinity binding to synapsin I in various phosphorylation states is characterized by a K_D in the region of 30 nM. Within the 'head' region there are apparently two sites that bind calmodulin.

Does calmodulin have the potential to regulate the activities of all synapsins, or is it a regulator of synapsin I only? To address this question, we have now examined binding of calmodulin to a representative of the synapsin II group, and to a *Drosophila* synapsin. Our data suggest that Ca^{2+}-dependent interaction with calmodulin is common to all synapsins.

MATERIALS AND METHODS

Reagents. cDNA encoding rat synapsin IIb (*1*) was generously provided by Dr. P. Greengard (Rockefeller University, New York). cDNA encoding *Drosophila* synapsin 1 (*6*) was generously given by Dr. Erich Buchner (Theodor Boweri Institute, University of Wurzburg, Germany): this cDNA (LcT 1−5/19 in the vector pGEXλT) contains base pairs 622−1970 of Dsyn-1. A Dsyn-1

† This work was supported by the Medical Research Council (U.K.). An equipment grant from the Wellcome Trust is acknowledged.

* To whom correspondence should be addressed. Telephone: +44 1227 823462. Fax: +44 1227 763912. Email: A.J.Baines@ukc.ac.uk.

⊗ Abstract published in *Advance ACS Abstracts,* August 15, 1997.

S0006-2960(97)00709-5 CCC: $14.00

fragment is expressed from this plasmid as a 79 kDa fusion with glutathione S-transferase.

Unphosphorylated synapsin I was purified as described previously (*10*).

Monoclonal antibodies SNH1 and SNT1 were used in Western blotting as previously described (*12*). Synthetic peptides were prepared by J. Hardy (University of Kent Protein Science Facility) using a Shimadzu peptide synthesizer. They were purified by HPLC, and their identities were confirmed by mass spectrometry.

Unless otherwise indicated, chemicals were obtained from Sigma Chemical Co. (Poole, Dorset, U.K.). Restriction and DNA ligase enzymes were from Boehringer Mannheim (Lewes, U.K.).

Preparation of Recombinant Rat Synapsin IIb. (A) Construction of a Bacterial Expression Vector for Rat Synapsin IIb. To express recombinant synapsin IIb, cDNA encoding full-length rat synapsin IIb was subcloned into the vector pET-23b (Novagen). Synapsin IIb cDNA was amplified from the original vector using polymerase chain reaction with Pfu polymerase (Stratagene) and the following primers: forward primer, CAAGCCATATGATGAACTTCCTGAG; reverse primer, GATCCTCGAGAGAAGCTTGGACTTG. The ATG within the *Nde*I site of the forward primer encodes codon 1 of synapsin IIb. Amplified cDNA was ligated into pET23b between *Nde*I and *Xho*I sites. In the resulting construct, codon 1 is the codon for initiation of translation, and the C-terminal of synapsin IIb is fused to $(his)_6$. The accuracy of the cDNA construct was confirmed by sequencing. This construct is designated pET23bS-IIb.

(B) Purification of Recombinant Rat Synapsin IIb. Recombinant his-tagged synapsin IIb was expressed in *E. coli* BL21(DE3) pLysS. Cells were cultured in LB AC broth (10g/L tryptone, 5 g/L yeast extract, and 5 g/L NaCl, pH 7.4) containing ampicillin (100 mg/L) and chloramphenicol (35 mg/L) at 37 °C to middle log phase. Cultures were then induced by the addition of isopropyl β-D-thiogalactopyranoside (IPTG)[1] to a final concentration of 0.8 mM and incubated for a further 4 h prior to being harvested by centrifugation. Cells were stored at −80 °C prior to use. Frozen cells were thawed on ice and resuspended in high-salt PBS (160 mM sodium phosphate, 4 M NaCl, pH 7.4) plus Complete protease inhibitors (Boehringer Mannheim, Lewes, U.K.). Recombinant synapsin IIb, recovered in the supernatant after centrifugation of lysed cells, was purified using the HisTrap purification kit (Pharmacia Biotech, St. Albans, U.K.) according to the manufacturer's recommended protocol. The resultant protein was dialyzed overnight at 4 °C against buffer A (150 mM NaCl, 10 mM Hepes/NaOH, 1 mM $CaCl_2$, 0.1% Tween 20, pH 7.4) and used within 48 h.

The purity of the preparations was verified by SDS−polyacrylamide gel electrophoresis (*13*). Synapsin IIb concentrations were determined spectrophotometrically, assuming an extinction coefficient of 44 600 M^{-1} cm^{-1}, estimated from the amino acid composition (*14*). The aggregation state was examined using calibrated sucrose gradient centrifugation (*15*).

(C) Phosphorylation of Synapsin IIb. Synapsin IIb was phosphorylated at Ser 10 using the catalytic subunit of cAMP-dependent kinase as described elsewhere for phosphorylation of synapsin I (*10*). The stoichiometry of phosphorylation was 0.8−0.9 mol of phosphate/mol of synapsin IIb.

Preparation of Recombinant Rat Synapsin IIb Fragments. To generate N-terminal and C-terminal portions of synapsin IIb, we took advantage of the unique *Nco*I site at codon 227. Recombinant synapsin IIb fragments containing residues 1−231 (N-terminal fragment) and 227−479 (C-terminal fragments) were produced. pET23bS-IIb construct was digested with *Nde*I and *Nco*I or *Nco*I and *Xho*I to remove the 5′ (codons 1−227) or 3′ (codons 228−479) regions of the synapsin IIb cDNA sequence, respectively. The remaining pET23b/partial synapsin IIb inserts were religated using oligonucleotide adaptors.

Recombinant His-tagged N- and C-fragments were expressed in *E. coli* BL21(DE3) pLysS. Cells were cultured in LB AC broth containing ampicillin (100 mg/L) and chloramphenicol (35 mg/L) at 37 °C to middle log phase. Cultures were then induced by the addition of IPTG to a final concentration of 1 mM and incubated for a further 4 h prior to harvesting by centrifugation. Cells were stored at −80 °C prior to use. The his-tagged protein was purified from inclusion bodies as follows. Cells were resuspended in high-salt PBS (pH 7.4) containing 4 M urea and 80 mM imidazole. Cell debris was removed by centrifugation (12000*g* for 10 min at room temperature) prior to being loaded onto a HisTrap chelating column. This was then washed with 20 column volumes of resuspension buffer prior to elution with high-salt PBS (pH 7.4) containing 2 M urea and 250 mM imidazole. Samples were then diluted (at least 100-fold) into buffer A prior to use.

Preparation of Recombinant Dsyn-1. cDNA encoding *Dsyn-1* (*6*) was transformed into *E. coli* strain JM109. Glutathione *S*-transferase (GST)−Dsyn-1, expressed as a 79 kDa GST−Dsyn-1 fusion protein, was purified from these bacteria by glutathione affinity chromatography.

Preparation and Covalent Modification of Calmodulin. Calmodulin was purified from sheep brain by methods described in Goold and Baines (*10*) that include the use of Ca^{2+}-dependent hydrophobic chromatography (*16, 17*). Calmodulin concentrations were estimated spectrophotometrically (*18*).

Biotinylated calmodulin was prepared using biotin-6-aminohexanoyl *N*-hydroxysuccinimide ester as described previously (*10*).

Calmodulin affinity columns were prepared using activated Sepharose CH-4B (Sigma) according to the manufacturer's instructions, using 2.5−3 mg of calmodulin/mL of swollen Sepharose.

Optical Biosensor Assays. Two optical biosensors were used in experiments reported here. One of the instruments was based upon the resonant mirror principle, the IAsys cuvette system (Affinity Sensors, Cambridge, U.K.). IAsys responses are measured in arc seconds (Arc S). The other was a surface plasmon resonance instrument (BIAcoreX, Pharmacia), responses from which are given in resonance units (RU). In both cases, biotinylated calmodulin was

[1] Abbreviations: buffer A, 150 mM NaCl, 10 mM Hepes/NaOH, 1 mM $CaCl_2$, 0.1% Tween 20, pH 7.4; buffer B, 150 mM NaCl, 20 mM Hepes/NaOH, 2 mM EGTA, 0.1% Tween 20, pH 7.4; EDC, 1-ethyl-3-[3-(dimethylamino)propyl]carbodiimide; IPTG, isopropyl β,D-thiogalactopyranoside; NHS, *N*-hydroxysuccinimide; PBS/Tween, 10 mM sodium phosphate, 150 mM NaCl, 0.05% Tween 20, pH 7.4; PO synapsin, unphosphorylated synapsin; PI synapsin, synapsin phosphorylated at site I; SDS, sodium dodecyl sulfate.

immobilized on the sensing surfaces using a biotin/streptavidin capture system. For the IAsys, approximately 20 ng/mm^2 of streptavidin was coupled to a (carboxymethyl)dextran cuvette using manufacturers' standard amine coupling protocol. Briefly, the cuvette was equilibrated with 10 mM sodium phosphate, 150 mM NaCl, 0.05% Tween 20, pH 7.4 (PBS/Tween), prior to activation of the carboxyl groups with a mixture of *N*-hydroxysuccinimide (NHS, 0.05 M final concentration) and 1-ethyl-3-[3-(dimethylamino)propyl]carbodiimide (EDC, 0.2 M final concentration) for 7 min. This was followed by two washes with PBS/Tween and two washes with 10 mM sodium acetate (pH 5.0). Streptavidin was added to a concentration of 100 μg/mL and incubated for 15 min. The surface was washed twice with PBS/Tween, and unoccupied carboxyl groups were blocked with 1 M ethanolamine (pH 8.5) for 2 min. After equilibration of the surface with PBS/Tween, the surface was washed twice with 20 mM HCl to remove noncovalently bound ligand prior to equilibration in buffer A. On the BIAcoreX, preprepared SA5 streptavidin-coupled chips were used. For the analysis of analytes >5 kDa in size, approximately 0.15−0.6 ng/mm^2 of biotinylated calmodulin was then captured upon the surface. For direct peptide analysis, approximately 2 ng/mm^2 calmodulin was captured upon an SA5 sensor chip. In all cases, varying concentrations of analyte in buffer A were used to investigate their interaction with the immobilized calmodulin ligand at 25 °C. Surfaces were regenerated by multiple washes with buffer B (150 mM NaCl, 20 mM Hepes/NaOH, 2 mM EGTA, 0.1% Tween 20, pH 7.4) followed by equilibration with buffer A prior to reuse.

Data Analysis. Kinetic constants were obtained from the IAsys sensor profiles by the use of Fast Fit software (Affinity Sensors). In the case of the BIAcore, kinetic constants were determined using either the BIAevaluation software (Pharmacia) or the nonlinear curve fitting program UltraFit (Biosoft, Cambridge, U.K.). Sensor profiles were overlaid using Microcal Origin 4.0 (Microcal, Northampton, MA).

Circular Dichroism. Assays were performed in a JASCO J-600 CD spectropolarimeter (20 °C, path length = 0.01 cm) using final concentrations of 10 μM calmodulin and 200 μM peptide in solutions containing 25 mM Tris/HCl, pH 7.4, 100 mM KCl, with either 0.5 mM Ca^{2+} or 2 mM EGTA. Blank spectra were generated using buffer plus peptide only. Spectra shown in this paper represent the average of 4 scans.

RESULTS

Recombinant Synapsin IIb. Rat synapsin IIb was expressed as a fusion with six histidine residues (a 'his-tag') at the C-terminus to aid purification. Purified recombinant synapsin IIb (Figure 1A) had the characteristics expected of the protein. The molecular mass determined by electrospray mass spectrometry was consistent with the predicted mass, and in sucrose gradient centrifugation it sedimented as a monomer (not shown). It was readily phosphorylated by cAMP-dependent protein kinase (Figure 1B).

The reaction of two anti-synapsin I monoclonal antibodies with recombinant synapsin IIb was also tested. SNH1 is a monoclonal antibody that recognizes an epitope in the first 50 amino acids of sheep synapsin I (*12*). The SNH1 epitope lies in the common 'head' region of all mammalian synapsins. Figure 1C shows that SNH1 recognized recombinant synapsin IIb in Western blots. SNT1, an anti-synapsin I antibody that recognizes the C-terminal 'tail' region of synapsin I, showed no reaction with synapsin IIb (Figure 1D), consistent with the lack of sequence identity between the short C-terminal tail of synapsin IIb (domains G and I) and the long C-terminal tail of synapsins Ia and Ib (domains D, E, F).

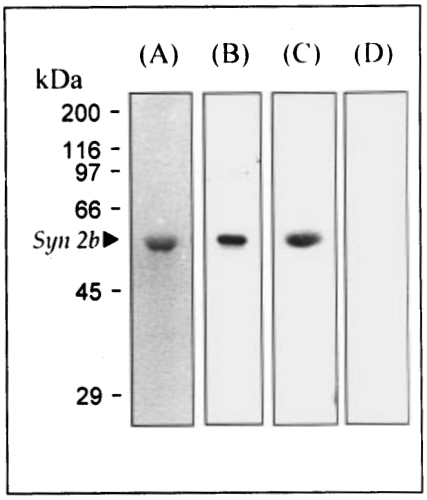

FIGURE 1: Recombinant synapsin IIb. Synapsin IIb was expressed in *E. coli* and purified as described in the text. The figure shows 10% polyacrylamide−SDS gels. (A) Purified synapsin IIb stained with Coomassie blue. (B) An autoradiograph of synapsin IIb labeled with ^{32}P after incubation with [γ-^{32}P]ATP and catalytic subunit of cAMP-dependent kinase. (C) A Western blot of synapsin IIb, showing reaction of monoclonal antibody SNH1. (D) Western blot showing no reaction with monoclonal antibody SNT1.

Ca^{2+}-Dependent Interaction of Synapsin IIb with Calmodulin in an Optical Biosensor. To investigate the possibility that synapsin IIb, like synapsin I, contains calmodulin binding sites, we employed an optical biosensor. An Affinity Systems IAsys resonant mirror biosensor was used. This instrument allows the interaction of molecules to be studied in real time (*19*).

To study the calmodulin−synapsin IIb interaction, a binding surface that would immobilize one of the partners was required. Methods for covalent modification of calmodulin are well established; therefore, we chose to immobilize calmodulin on the surface of an IAsys cuvette, and follow the interaction of synapsin IIb added in solution to the cuvette. To prepare the cuvette for immobilization of calmodulin, streptavidin was coupled to a carboxymethylated dextran cuvette surface using NHS/EDC (see Materials and Methods). Unbound streptavidin was removed, and biotinylated calmodulin was added. The biotinylated calmodulin was captured by the streptavidin and formed a stable surface. Washing the surface with either Ca^{2+}-containing or EGTA-containing buffers showed <0.05% of the calmodulin lost over 20 min. Note also that biotinylated calmodulin with a hexanoic acid spacer arm has been shown to retain full biological activity when bound to avidin (*20*).

Figure 2A shows the time course of interaction of unphosphorylated synapsin IIb added in solution to the calmodulin surface in an IAsys cuvette. Synapsin IIb bound to the calmodulin surface in a Ca^{2+}-containing buffer (buffer A). For a solution of 47 nM synapsin IIb, binding was essentially complete in 5 min. Free synapsin IIb was removed by washing with buffer A: slow dissociation was observed. When the buffer was changed to one that contained EGTA (buffer B), a rapid decrease in signal was

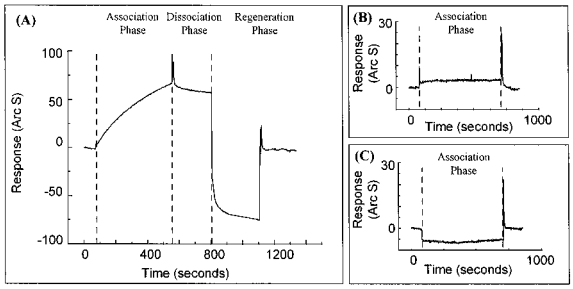

FIGURE 2: Ca^{2+}-dependent binding of recombinant synapsin IIb to immobilized biotinylated calmodulin. To generate the binding surface, streptavidin was coupled to a carboxylated dextran surface in an IAsys resonant mirror cuvette (Affinity Instruments). This was then used to capture biotinylated calmodulin. The captured calmodulin was washed in buffer A (see Materials and Methods). At the time indicated by the first vertical dashed line in (A), synapsin IIb was added to a final concentration of 47 nM (reaction volume 200 μL). Binding was detected by a change in the resonance angle. At the point indicated by the second dashed line, unbound synapsin IIb was removed, and the incubation was continued with buffer A alone. The dissociation of bound synapsin IIb (slow drop in the trace) was followed, until the point indicated by the third dashed line. At this point, buffer A was removed, and replaced with buffer B to remove remaining bound synapsin IIb and regenerate the calmodulin surface. The sharp drop follows the inactivation of calmodulin, and consequent dissociation of bound synapsin IIb; part of the observed drop also derives from a change in refractive index in the solution. Replacing buffer B with buffer A reveals that the bound synapsin IIb has dissociated: note that the base line has returned to zero. (B) Binding was not observed in Ca^{2+}-containing buffer A in the presence of trifluoperazine, a calmodulin inhibitor. (C) Synapsin IIb added to the calmodulin surface in the presence of buffer B showed no binding, again indicating that the binding is Ca^{2+}-dependent.

noted. In part this originated in the differences in refractive index between buffers A and B, but most of the decrease derived from the inactivation of calmodulin in buffer B, and the consequent dissociation of synapsin IIb from the surface.

Figure 2B,C indicates the requirement for active calmodulin in the interaction. No interaction took place if the calmodulin inhibitor trifluoperazine was added to buffer A (Figure 2A), nor in the presence of EGTA (buffer B, Figure 2C). No interaction of synapsin IIb was observed with the streptavidin-coated surface (not shown).

Quantification of the Interaction of Synapsin IIb with Calmodulin. To quantify the interaction, the experiment was repeated with different concentrations of synapsin IIb in phosphorylated (PI) and unphosphorylated (PO) states. Figure 3A shows the association and dissociation phases of PI and PO synapsin IIb on the same cuvette surface. PI synapsin appeared to associate and dissociate much faster than PO. Figure 3B,C shows the observed rates of association for each form as a function of synapsin concentration. For both PI and PO synapsin IIb, the association phases of the interaction were not well described by equations for single phase association kinetics: there appeared to be more than one association reaction. The association data were described accurately by equations for biphasic kinetics, one with a much faster association phase then the other. Such biphasic reaction kinetics are often seen in optical biosensor assays [see (*21*) for example]. The origin of the second (slower) association phase is unclear, and could arise from artifacts (see Discussion), so only data for the faster association phase are shown here. Table 1 summarizes the rate constants for the derived fast association phase with synapsin IIb. The differences in the apparent association

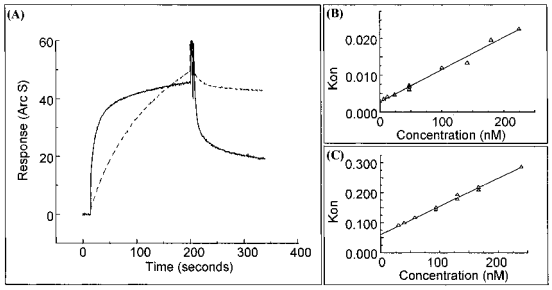

FIGURE 3: Analysis of synapsin IIb−calmodulin interaction. (A) The association and dissociation phases of phosphorylated (solid line) and unphosphorylated (dashed line) 80 nM synapsin IIb with a calmodulin surface. Note the much more rapid nature of both phases with phosphorylated (PI) synapsin IIb. (B) Unphosphorylated synapsin IIb was added to an immobilized calmodulin surface over a range of concentrations up to 200 nM. For each reaction, the observed on rate constant, K_{on}, was calculated using FASTFIT. A plot of K_{on} against concentration gives K_{ass} (gradient of the line)- and K_{diss} (from the extrapolated *y*-intercept). The figure shows a line calculated for K_{ass} and K_{diss} values shown in Table 1. (C) A plot of K_{on} against the concentration of PI synapsin IIb is shown. The figure shows a line calculated for K_{ass} and K_{diss} values shown in Table 1. See the text for a description of the derivation of K_{on}.

Table 1: Characteristics of Calmodulin Interactions with Synapsins

protein	K_{ass} (M^{-1} s^{-1})	K_{diss} (s^{-1})	K_D (nM)
PO synapsin IIb	$8.75 \times 10^4 \pm 3.61 \times 10^3$	$2.67 \times 10^{-3} \pm 3.96 \times 10^{-4}$	31 ± 5
PI synapsin IIb	$9.14 \times 10^5 \pm 3.16 \times 10^4$	$5.37 \times 10^{-2} \pm 3.90 \times 10^{-3}$	59 ± 5
PO synapsin I	$8.18 \times 10^4 \pm 1.06 \times 10^3$	$1.55 \times 10^{-3} \pm 8.21 \times 10^{-4}$	19 ± 10
GST−dsynapsin II	$2.43 \times 10^4 \pm 4.31 \times 10^3$	$2.91 \times 10^{-3} \pm 3.14 \times 10^{-4}$	120 ± 25

[a] The table summarizes the kinetic characteristics of the interaction with calmodulin determined for different synapsins.

and dissociation rates between PI and PO synapsin IIb (indicated in Figure 2) were reflected in the observed forward (K_{ass}) and reverse (K_{diss}) rate constants for calmodulin−synapsin IIb interaction: these were changed by an order of magnitude for the former, and by a factor of 20 for the latter (see Table 1). To confirm the values for K_{diss}, a separate plot of apparent K_{diss} determined at each synapsin IIb concentration (not shown) gave a value for K_{diss} that was (within the limits of error) indistinguishable from the values shown in Table 1.

From the rate constants, the K_D values were calculated ($K_D = K_{diss}/K_{ass}$). The strong class fitted well to K_D 31 ± 5 nM for PO synapsin IIb and 59 ± 5 nM for PI synapsin IIb. To ensure internal consistency of the data (*22*), K_D values were also calculated from the extent of binding at different synapsin concentrations (not shown). From these data, K_D values of 29 ± 9 nM for PO synapsin IIb and 54 ± 3 nM for PI synapsin IIb were derived.

The effect of phosphorylation on synapsin IIb−calmodulin interaction is to make the overall reaction much faster, but with only a moderate change in affinity.

For comparison with synapsin IIb, we also assayed the interaction of unphosphorylated synapsin I using the IAsys biosensor. Table 1 gives the results of these experiments. The association and dissociation rate constants for synapsin I were very similar to those determined for synapsin IIb. The K_D values for unphosphorylated synapsin I in the biosensor system were 19 ± 10 nM (from the rate constants)

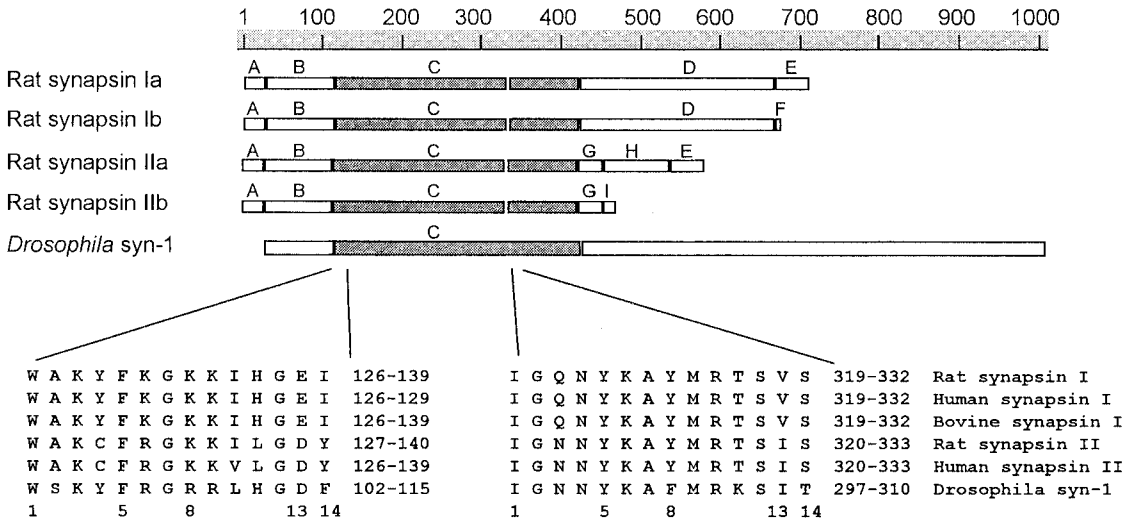

FIGURE 4: Sequences of synapsins indicate two potential calmodulin binding sites. The figure shows alignments of synapsin sequences generating using BLOSUM 62 in MACAW (*40*). Top: alignments of the domains of rat synapsins (*1*) and the long form of Dsyn-1 (*6*). The domains of the mammalian synapsins are lettered. The most highly conserved domain, C, is shaded: a break has been introduced into the sequence of mammalian domain C for best alignment with Dsyn-1 C. Bottom: the sequences of the potential calmodulin binding sites in several mammalian synapsins and in Dsyn-1 are shown aligned with each other. The numbering below the sequences indicates the positions of key residues in a 14 amino acid pattern identified as potentially critical to calmodulin binding. For a discussion of these sequences, see the text.

and 20 ± 7 nM (from the extent of binding). This agrees well with previous work (*10*) using an independent method (fluorescence enhancement) which gave K_D 36 ± 14 nM.

N- and C-Terminal Portions of Synapsin IIb Each Contain Calmodulin Binding Sites. There is good evidence that synapsin I has two nonoverlapping calmodulin binding sites, although the binding is best described by a single high-affinity class of interaction [see (*10*) and data above]. Because of the sequence similarity with the head region of synapsin I, it is possible that synapsin IIb might have two distinct regions of sequence that bind calmodulin.

To test this, two constructs were prepared that represent different regions of synapsin IIb. Goold and Baines (*10*) noted that synapsin I had two regions of sequence that bound calmodulin: one was located in a 7.4 kDa proteolytic fragment beginning at residue 62; the other was within a 6.5 kDa fragment beginning at 288. In the synapsin IIb cDNA, there is a unique *Nco*I restriction site at codon 227. Digestion of the cDNA at this point was used to generate cDNAs encoding N-terminal and C-terminal portions of the protein (1−231 and 228−479, respectively). N-terminal and C-terminal fragments were expressed in *E. coli*.

The two fragments were difficult to purify and analyze. Both were found in inclusion bodies within the bacteria and were purified on a chelating column in the presence of urea. The fragments were insoluble after dialysis to remove the urea. However, low concentrations of material were obtained for testing of a binding activity by diluting the urea-containing protein solution with buffer A, although the concentrations obtained were insufficient for a fully quantified analysis. Each fragment bound to calmodulin in a biosensor (data not shown). The binding was Ca^{2+}-dependent. In these experiments, residual urea concentrations were 20 mM. The N-terminal fragment showed a much faster association rate and a slower dissociation rate in buffer A than the C-terminal fragment.

These data are consistent with the existence of two different regions of sequence in synapsin IIb that bind calmodulin, the N-terminal region presumably having the higher affinity.

Identification of Possible Calmodulin Binding Sites in the Synapsin IIb Sequence. Calmodulin recognizes regions of sequence exposed on protein surfaces that are often described as basic amphiphilic α-helices (*23*). Erickson-Viitanen and DeGrado (*24*) have quantified the hydrophobicity and helical hydrophobic moment associated with several calmodulin binding sequences. Crivici and Ikura (*25*) have described a pattern of 14 residues found within calmodulin targets. The sequences of mammalian synapsins were analyzed for regions of sequence that fit to the Erickson-Viitanen and Crivici parameters. Two sequences were found—these are residues 127−140 and 320−333 in synapsin IIb.

For residues 127−140, the Erickson-Viitanen values were the following: hydrophobic index (*26*), −0.1; charge, +3; helical hydrophobic moment, 0.30 (*24*). For 320−333, the values were as follows: hydrophobicity, −0.07; charge, +2; helical hydrophobic moment, 0.17. For comparison, the typical range of calmodulin binding sequences (in proteins or peptides with K_D 0.1−790 nM) is the following: hydrophobicity, −0.3 to +0.3; charge, 0 to +5; helical hydrophobic moment, 0.16−0.6. Figure 4 indicates that similar regions are found in all published synapsins.

Crivici and Ikura (*25*) described a pattern of residues reflecting the interaction of the major hydrophobic and basic anchors with calmodulin. Since calmodulin is flexible, the pattern is rarely precisely followed in any one sequence. In general, the preferences in this pattern are that the first residue is hydrophobic, the fifth is hydrophobic (or basic), the eighth is hydrophobic (or occasionally charged), the thirteenth is basic (but it can be another hydrophilic, or strongly hydrophobic residue), and the fourteenth is hydrophobic (less often hydrophilic). The overall patterns of residues in the two regions are consistent with calmodulin binding sequences, but the acidic residue at the thirteenth position in the first of the sequences is atypical.

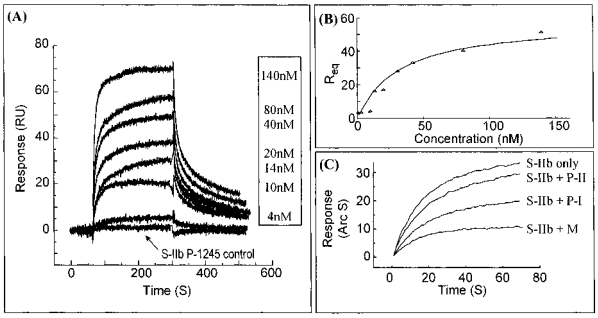

FIGURE 5: High-affinity interaction of synapsin IIb peptide 1 with calmodulin. (A) Surface plasmon resonance analysis showing sensorgrams over a range of peptide concentrations (4−140 nM). A control peptide, residues 462−476 of synapsin IIb, showed no binding at a concentration of 100 nM. (B) Analysis of the interaction between synapsin IIb peptide I and calmodulin. A plot of steady-state binding levels (R_{eq}, relative response at equilibrium) against concentration of peptide is shown. The curve shown is calculated for an apparent K_D = 32 nM. (C) Resonant mirror analysis of the competition between recombinant synapsin IIb and calmodulin binding peptides for calmodulin on the cuvette surface. A biotin−calmodulin surface was equilibrated with 500 nM of the indicated peptide in buffer A (total volume 180 μL). 20 μL of synapsin IIb/peptide mixture (final concentrations of 50 nM and 1 μM, respectively). Responses were normalized and percentage inhibitions calculated with respect to 50 nM synapsin IIb only. peptide I (P-I), 42% inhibition; Peptide II (P-II), 12% inhibition; and mastoparan (M), 70% inhibition.

Interaction of Peptides Representing Residues 122−143 and 313−334 with Calmodulin. Although Crivici and Ikura identified a pattern of 14 residues that are critical for calmodulin binding, residues outside the 14 residue sequence also interact with calmodulin. Peptides representing residues 122−143 (peptide 1) and 313−334 (peptide 2) were synthesized, and tested for binding to calmodulin. In initial experiments, binding was tested by native gel electrophoresis (*24*). Peptide 1 bound calmodulin in native gels in the presence of Ca^{2+}, but not in the presence of EGTA (data not shown). No interaction with calmodulin was detected with peptide 2.

Figure 5 shows optical biosensor profiles for the interaction of peptide 1 with calmodulin. Peptide 1 bound to calmodulin (Figure 5A,B). The K_D was 32 ± 10 nM. A control peptide (synapsin IIb 462−476) showed no interaction in this system (Figure 5A). No binding of peptide 1 to the surface was observed in EGTA (data not shown). To ensure that peptide 1 bound in the active site of calmodulin, and did not simply show a nonspecific interaction with calmodulin, it was tested as a competitor of calmodulin binding to synapsin IIb. The optical biosensor measures the mass of material bound to a surface; therefore, competitive inhibition of (relatively high molecular mass) synapsin IIb binding to calmodulin by (relatively low molecular mass) peptides will be detected as a reduction in the biosensor response. Figure 5C shows that addition of peptide 1 gave a reduction in the biosensor response when synapsin IIb was added. As a control, the bee venom peptide mastoparan was used for comparison. Mastoparan also inhibited binding. Mastoparan binds to calmodulin with higher affinity [K_D 0.3 nM (*27*)] than the synapsin peptide, and so appears to be a more effective inhibitor.

Peptide 2, by contrast, bound calmodulin weakly. In the peptide competition assay, under the conditions shown in Figure 5C, it displaced only 12% of the synapsin binding.

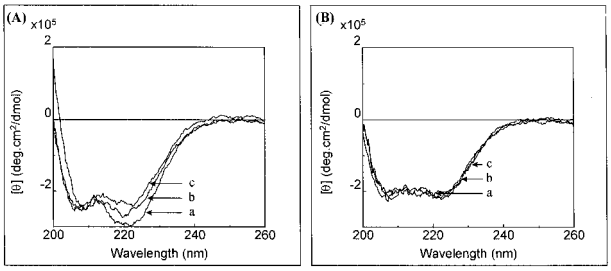

FIGURE 6: Far-UV circular dichroism spectra of unmodified calmodulin with synapsin IIb peptides I and II. Far-UV circular dichroism spectra of (A) calmodulin in the presence of Ca^{2+} and (B) calmodulin in the presence of EGTA. Trace a shows spectra obtained in the presence of peptide 1; trace b shows spectra obtained in the presence of peptide 2; trace c shows spectra obtained in the absence of added peptide. In each case, the spectra were obtained by subtracting corresponding buffer or peptide solution blanks. Note that peptide 1 gives the greatest Ca^{2+}-dependent change in the CD spectrum of calmodulin.

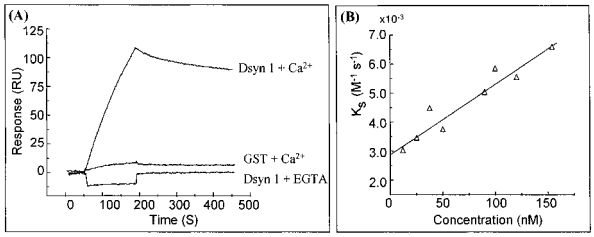

FIGURE 7: Ca^{2+}-dependent binding of Dsyn-1 to calmodulin. (A) Surface plasmon resonance analysis of the interaction of Dsyn-1 (final concentration 160 nM) performed over a biotinn-calmodulin surface (SA 5 Biacore sensor chip, Pharmacia) compared to a streptavidin surface reveals a calcium-dependent interaction. Injection of glutathione *S*-transferase (160 nM) gave a negligible response compared to the intact fusion protein. (B) Analysis of the interaction of Dsyn-1 with calmodulin. A monophasic model was used, and values for K_s ($K_s = K_{ass}$[free analyte] + K_{diss}) were determined over a range of concentrations. A plot of K_s against the concentration of Dsyn-1 is shown, with a line calculated for K_{ass} and K_{diss} values shown in Table 1.

For comparison, peptide 1 and mastoparan gave 42% and 70% inhibition, respectively. The binding of peptide 2 was too weak for us to determine a K_D in an optical biosensor.

Peptide 1 was also analyzed by circular dichroism spectroscopy. In buffer A, little α-helical content was found, although in a more hydrophobic solvent, the peptide had an α-helical content (not shown). Figure 6 shows that peptide 1 increased the α-helical content of calmodulin in the presence of Ca^{2+}. These data are consistent with peptide 1 causing the expected conformational change in Ca^{2+}/calmodulin on binding. The CD spectra give a marginal indication of an interaction of peptide 2 with calmodulin (Figure 6).

Peptide 1 has the characteristics expected of the high-affinity calmodulin binding site in synapsin IIb.

Dsyn-1 Interacts with Calmodulin. Comparison of published synapsin sequences indicated that Dsyn-1 should also bind synapsin. A Dsyn-1 fragment, encoded by base pairs 622−1970, was expressed as a GST fusion protein from a plasmid described by Klagges et al. (*6*).

In initial experiments, the Dsyn-1 fragment was tested for binding to calmodulin by affinity chromatography (data not shown). The column bound the fragment in the presence of Ca^{2+} (buffer A), and it was recovered after washing the column with EGTA (buffer B). Figure 7A shows that Dsyn-1 gave Ca^{2+}-dependent binding to mammalian calm-

odulin. The interaction was quantified (Figure 7B) and conformed to a single class of binding site, K_D 120 nM. These data indicate that binding of calmodulin to synapsins is conserved in an invertebrate. Note also that the fusion partner, GST, showed no significant interaction with calmodulin (Figure 7A).

DISCUSSION

The effects of multiple kinases (*28*−*31*) and of calmodulin (*10*, *11*) on the actin binding activities of synapsin I have been well documented. In general, both are inhibitors of the activity, and each reinforces the other. However, not all the kinases that phosphorylate synapsin I (e.g., calmodulin-dependent protein kinase II) also phosphorylate the synapsin II proteins. Likewise, the well-characterized phosphorylation sites for kinases such as calmodulin-dependent protein kinase II are not conserved in the *Drosophila* synapsins (*6*). By analogy with phosphorylation, is it the case that calmodulin (like kinase II) is only a regulator of synapsin I, or is it a fundamental aspect of the regulation of synapsin activities?

In addressing this question, we have provided evidence that calmodulin binding is conserved in mammalian synapsins I and II (Figures 2 and 3), and in an insect synapsin (Figure 7). This indicates that calmodulin binding is a fundamental characteristic of synapsins. Residues 121−143 are recognized by calmodulin with a K_D that is indistinguishable from that of the native protein (Figure 5), and similar sequences are found in all synapsins (Figure 4). In addition to these points, we also provide evidence that phosphorylation at Ser 10 of rat synapsin IIb has a substantial effect on the association and dissociation rate constants (Figure 3 and Table 1).

Synapsin IIb has been referred to as a 'minimal' synapsin, containing the N-terminal 'head' region common to all mammalian synapsins with a very short C-terminal tail (*1*). We considered this an appropriate representative of the synapsin II family in these experiments because it retains the conserved activities and regulation typical of synapsins: it binds actin and synaptic vesicle sites (*32*), and Ser 10 is phosphorylated by cAMP-dependent kinase and calmodulin-dependent protein kinase I (*1*, *33*). Moreover, all the Ca^{2+}-dependent binding of calmodulin to synapsin I occurs in the head region (*9*, *10*). Note also that the amino acid sequences of the head regions of synapsin IIa and IIb are encoded by the same gene (*1*).

Synapsin IIb is a challenging molecule to analyze. Even starting with large quantities of brain, it is only obtainable in microgram quantities (*34*). In preliminary experiments (N. V. L. Hayes and A. J. Baines, data not shown), synapsin IIb isolated from brain showed Ca^{2+}-dependent binding to calmodulin affinity columns, but the amounts obtainable were well below those required for a quantified analysis. A recombinant source of the protein was clearly required for the purposes of this paper. Although it is always a concern that a heterologous protein folds correctly when expressed in bacteria, we considered bacterial expression suitable for several reasons. First, Thiel et al. (*32*) showed that it was possible to analyze activities of synapsin IIb expressed in bacteria: their experiments give confidence that the native binding activities of the protein are retained in the recombinant protein. Second, intact synapsin IIb used in these experiments was purified from the soluble portion of a bacterial extract, and did not need to be refolded from inclusion bodies. Third, the purified protein showed the expected characteristics: it was a monomer, readily phosphorylated by cAMP-dependent kinase (Figure 1), and it also had an actin binding activity (data not shown). Finally, the close values obtained for the apparent K_D for binding calmodulin of both synapsin I (obtained from brain) and recombinant synapsin IIb are consistent with correct folding.

In synapsin I, two separate calmodulin binding sites have been detected, both within the head region (*10*). On the other hand, there is just one dominant affinity of binding: this would imply either that both sites have indistinguishable affinities, or that one is so much lower than the other that it was not detected in the fluorescence enhancement assay (*10*). Results reported here for synapsin IIb show a similar pattern. Like synapsin I, the binding curves for synapsin IIb are dominated by a single affinity class, with an overall K_D of ∼31 nM (Figures 2 and 3, and Table 1). This is close to the ∼36 nM reported previously for synapsin I in a fluorescence enhancement assay (*10*), and not very different from the value determined here using a biosensor (Table 1).

In the binding data (derived from those indicated in Figures 2 and 3), there was a suggestion that a second affinity class, some 3−5-fold weaker than the 31 nM site, was present in synapsins I and IIb (not shown). However, it is a major limitation of current optical biosensor technology that it is not possible to state that this lower class of affinity was in any way related to binding of calmodulin to the C-terminal region of synapsin IIb. In the biosensor experiments reported here, calmodulin was immobilized in the biosensor via a biotin link to streptavidin, itself covalently coupled to a dextran-coated binding surface. Artifacts that can arise in this system include steric hindrance of the active site in a subpopulation of calmodulin, partial denaturation, mass transport effects, and rebinding of ligands during the dissociation phase (*21*, *22*, *35*). For these reasons, we prefer not to place emphasis on the slower component of a biosensor assay. To control for some of these effects, several additional controls were done (data not shown). Surfaces were coupled at different calmodulin densities (to address the issues of mass transport and steric hindrance), and unbiotinylated calmodulin was added in some instances during the dissociation phases to examine the possibility of rebinding. No evidence for rebinding during the dissociation phase was noted, and at several different coupling densities, biphasic reaction kinetics were observed. Nevertheless, given the limitations of the optical biosensor methodology, it would be premature to state that the slower reaction represents a second (lower affinity) site. A further point to note is that the difference in observed rate constants for phosphorylated and unphosphorylated synapsin IIb did not arise from the use of different sensor surfaces: phosphorylated and unphosphorylated synapsin IIb reproducibly gave different observed association rates when analyzed on the same calmodulin surface.

Given the presence of a K_D ∼30 nM site in mammalian synapsins, what is its identity? The stronger portion of synapsin IIb interaction with calmodulin is likely to reside in residues 1−228. In synapsin I, a 7.5 kDa peptide starting at residue 62 (derived from a V8 protease digest of synapsin I) was isolated from a calmodulin affinity column (*10*). Examining the sequence of synapsins I and II, we could only

find one potential calmodulin binding site within residues 62−228. Using hydrophobicity, helical hydrophobic moment, and charge characteristics (*24*) as well as the overall pattern of residues (*25*), sequence 126−139 was identified (Figure 4). The K_D of peptide 1 for synapsin (∼32 nM, Figure 5) is essentially the same as that of the whole unphosphorylated protein, which gives some confidence that this peptide represents the native calmodulin binding site.

One unusual aspect of sequence 126−139 is the presence of a glutamate residue at 13 in the pattern. It is rare, but not unique, to find an acidic residue in a calmodulin binding sequence: both caldesmon and phosphorylase kinase contain acidic residues in their calmodulin binding sites (*25*).

In aqueous buffer, circular dichroism spectroscopy indicated that peptide 1 (121−143) had little secondary structure, although a helical component was revealed in a more hydrophobic solution (data not shown). This is similar to several other calmodulin binding peptides [e.g., (*36*)]. Certainly the peptide binds to calmodulin at the active site, since it both inhibited binding of whole synapsin IIb (Figure 5C) and caused an increase in the helicity of calmodulin (Figure 6).

Table 1 indicates that the interaction of calmodulin with phosphorylated synapsin IIb (PI synapsin IIb) is weaker by a factor of ∼2 compared to the unphosphorylated protein, but more rapid by an order of magnitude or more. Presumably this reflects a conformational change in synapsin IIb. This suggestion is supported by studies of intrinsic fluorescence (*37*) and observations of different fluorescent yields of AEDANS-calmodulin bound to synapsin I in different phosphorylation states (*10*). Perhaps in the phosphorylated protein the calmodulin binding site is more exposed to the surface, but in a conformation slightly less favorable for binding. Greater accessibility of the site may be reflected in the observation that PI synapsin I is more susceptible to the inhibition of actin bundling by calmodulin than PO synapsin I (*11*), even though the affinity of the two forms of synapsin I for calmodulin is not significantly changed. It will clearly be of importance to clarify this experimentally.

The nature of the interaction of the C-terminal region of synapsin IIb remains more equivocal. The C-terminal fragment (residues 227−479) bound to calmodulin, but apparently weakly. This agrees with observations on synapsin I: a 6.5 kDa proteolytic fragment starting at residue 288 of synapsin I was isolated from a calmodulin affinity column (*10*). This may indicate a lower limit for the K_D of the interaction at about 1 μM, the conventional lower limit for affinity chromatography (*38*). Peptide 2 (residues 313−334) was (on the basis of sequence analysis) the best candidate for a calmodulin binding site in this region, and its interaction with calmodulin is seemingly weak (Figures 5 and 6). Whether binding of calmodulin to 313−334 is physiologically significant remains unclear.

Finally, we note that Dsyn-1 binds mammalian calmodulin (Figure 7). In the biosensor assay, the interaction was relatively weak (K_D ∼120 nM). This measurement must be qualified by noting the heterologous components of the reaction, and the N-terminal GST fusion partner which has, under certain conditions, been shown to self-associate in biosensor assays (*39*). However, the data confirm that calmodulin binding is conserved across the synapsins during evolution.

ACKNOWLEDGMENT

We thank Dr. Steve Mayes of Affinity Sensors for help with the IAsys methodology and interpretation of data.

REFERENCES

1. Sudhof, T. C., Czernik, A. J., Kao, H. T., Takei, K., Johnston, P. A., Horiuchi, A., Kanazir, S. D., Wagner, M. A., Perin, M. S., De Camilli, P., and Greengard, P. (1989) *Science 245*, 1474−1480.
2. Rosahl, T. W., Spillane, D., Missler, M., Herz, J., Selig, D. K., Wolff, J. R., Hammer, R. E., Malenka, R. C., and Sudhof, T. C. (1995) *Nature 375*, 488−493.
3. Li, L., Chin, L. S., Shupliakov, O., Brodin, L., Sihra, T. S., Hvalby, O., Jensen, V., Zheng, D., McNamara, J. O., Greengard, P., and Andersen, P. (1995) *Proc. Natl. Acad. Sci. U.S.A. 92*, 9235−9239.
4. Takei, Y., Harada, A., Takeda, S., Kobayashi, K., Terada, S., Noda, T., Takahashi, T., and Hirokawa, N. (1995) *J. Cell Biol. 131*, 1789−1800.
5. Ferreira, A., Han, H. Q., Greengard, P., and Kosik, K. S. (1995) *Proc. Natl. Acad. Sci. U.S.A. 92*, 9225−9229.
6. Klagges, B. R. E., Heimbeck, G., Godenschwege, T. A., Hofbauer, A., Pflugfelder, G. O., Reifegerste, R., Reisch, D., Schaupp, M., Buchner, S., and Buchner, E. (1996) *J. Neurosci. 16*, 3154−3165.
7. Hirokawa, N., Sobue, K., Kanda, K., Harada, A., and Yorifuji, H. (1989) *J. Cell Biol. 108*, 111−126.
8. Sudhof, T. C. (1995) *Nature 375*, 645−653.
9. Hayes, N. V. L., Bennett, A. F., and Baines, A. J. (1991) *Biochem. J. 275*, 93−97.
10. Goold, R., and Baines, A. J. (1994) *Eur. J. Biochem. 224*, 229−240.
11. Goold, R., Chan, K. M., and Baines, A. J. (1995) *Biochemistry 34*, 1912−1920.
12. Nicol, S., Chan, K.-M., and Baines, A. J. (1994) *Biochem. Soc. Trans. 22*, 52S.
13. Laemmli, U. K. (1970) *Nature 227*, 680−685.
14. Pace, C. N., Vajdos, F., Fee, L., Grimsley, G., and Gray, T. (1995) *Protein Sci. 4*, 2411−2423.
15. Martin, R. G., and Ames, B. N. (1961) *J. Biol. Chem. 236*, 1372−1379.
16. Gopalakrishna, R., and Anderson, W. B. (1982) *Biochem. Biophys. Res. Commun. 104*, 830−836.
17. Dedman, J. R., and Kaetzel, M. A. (1983) *Methods Enzymol. 102*, 1−8.
18. Jarrett, H. W., and Penniston, J. T. (1977) *J. Biol. Chem. 253*, 4676−4682.
19. Cush, R., Cronin, J. M., Stewart, W. J., Maule, C. H., Molloy, J., and Goddard, N. J. (1993) *Biosensors Bioelectronics 8*, 347−353.
20. Polli, J. W., and Billingsley, M. L. (1991) *Biochem. J. 275*, 733−743.
21. Edwards, P. R., Gill, A., Pollardknight, D. V., Hoare, M., Buckle, P. E., Lowe, P. A., and Leatherbarrow, R. J. (1995) *Anal. Biochem. 231*, 210−217.
22. Schuck, P., and Minton, A. P. (1996) *Trends Biochem. Sci. 21*, 458−460.
23. O'Neill, K. T., and DeGrado, W. F. (1990) *Trends Biochem. Sci. 15*, 59−64.
24. Erickson-Viitanen, S., and DeGrado, W. F. (1987) *Methods Enzymol. 139*, 455−478.
25. Crivici, A., and Ikura, M. (1995) *Annu. Rev. Biophys. Biomol. Struct. 24*, 85−116.
26. Eisenberg, D., Schwartz, E., Komaromy, M., and Wall, R. (1984) *J. Mol. Biol. 179*, 125−142.
27. Malencik, D. A., and Anderson, S. R. (1983) *Biochem. Biophys. Res. Commun. 114*, 50−56.
28. Bahler, M., and Greengard, P. (1987) *Nature 326*, 704−707.
29. Petrucci, T. C., and Morrow, J. S. (1987) *J. Cell Biol. 105*, 1355−1363.

30. Matsubara, M., Kusubata, M., Ishiguro, K., Uchida, T., Titani, K., and Taniguchi, H. (1996) *J. Biol. Chem. 271*, 21108−21113.
31. Jovanovic, J. N., Benfenati, F., Siow, Y. L., Sihra, T. S., Sanghera, J. S., Pelech, S. L., Greengard, P., and Czernik, A. J. (1996) *Proc. Natl. Acad. Sci. U.S.A. 93*, 3679−3683.
32. Thiel, G., Sudhof, T. C., and Greengard, P. (1990) *J. Biol. Chem. 265*, 16527−16533.
33. Czernik, A. J., Pang, D. T., and Greengard, P. (1987) *Proc. Natl. Acad. Sci. U.S.A. 84*, 7518−7522.
34. Huang, C. K., Browning, M. D., and Greengard, P. (1982) *J. Biol. Chem. 257*, 6524−6528.
35. Nieba, L., Krebber, A., and Pluckthun, A. (1996) *Anal. Biochem. 234*, 155−165.
36. Buku, A., Probst, W. C., Weiss, K. R., and Heierhorst, J. (1996) *Biochem. Biophys. Res. Commun. 218*, 854−859.
37. Benfenati, F., Neyroz, P., Bahler, M., Masotti, L., and Greengard, P. (1990) *J. Biol. Chem. 265*, 12584−12595.
38. Scopes, R. K. (1982) *Protein Purification: principles and practise*, Springer-Verlag, New York.
39. Marfatia, S. M., Cabral, J. H. M., Lin, L. H., Hough, C., Bryant, P. J., Stolz, L., and Chishti, A. H. (1996) *J. Cell Biol. 135*, 753−766.
40. Schuler, G. D., Altschul, S. F., and Lipman, D. J. (1991) *Proteins: Struct., Funct., Genet. 9*, 180−190.

BI970709R